Journal of Radiotherapy in Practice

Journal of Radiotherapy in Practice (2006)
5, 121–128

doi: 10.1017/S1460396906000161

Original Article

Improved peripheral dose calculation accuracy for a small MLC field brought by the latest commercial treatment planning system

J. C. L. Chow[1,2], G. N. Grigorov[3], R. Jiang[2,3]

[1]*Princess Margaret Hospital, University Health Network, Ontario,* [2]*Physics Department, University of Waterloo, Ontario,* [3]*Medical Physics Department, Grand River Hospital, Ontario, Canada*

Abstract

A recently released Pinnacle treatment planning system software, v7.4f includes some new physics features such as modeling of the rounded multi-leaf collimator (MLC) leaf ends and the tongue-and-groove structure between leaves. In this study, the above physics modeling improvements were verified by comparing the peripheral dose profiles for the small MLC fields calculated by the new Pinnacle v7.4f and the old Pinnacle v6.2b with those obtained from measurements experimentally. Three test MLC fields with different jaw sizes were prepared, and specific dose profiles (along cross-line, in-line and diagonal axis) at different depths were measured using a Varian 21 EX linear accelerator with 120-leaf Millennium MLC, big scanning water tank and photon diode. Estimated dose profiles for the test fields were calculated using Pinnacle v6.2b and v7.4f. By comparing the measured and calculated results, it was found that both v6.2b and v7.4f performed well in calculating the cross-line (along the gap between the longitudinal lengths of two leaves) and diagonal axis dose profiles at different depths. However, v7.4f gave calculated dose values closer to the measured field for in-line (gap between junctions of two rounded leaf ends) axis dose profiles at different depths. For the shape of the profile along the in-line axis, v7.4f calculated a flat "platform" dose profile of about 34.3% (inter-bank leakage) at depth d_{max} beyond the MLC field edge using a clinical dose grid size of $0.4 \times 0.4 \times 0.4\,cm^3$, compared to the "zigzag" dose profile varying between 35.4% and 42.1% measured using the water tank and diode. However, both Pinnacle v6.2b and v7.4f calculated the percentage depth dose for the test fields well compared to the measurements.

Keywords

Intensity modulated radiotherapy; multi-leaf collimator; treatment planning software commissioning and dosimetry

INTRODUCTION

The dosimetry of step-and-shoot intensity modulated radiotherapy (IMRT) fields is more complicated than conventional radiotherapy because the beam intensity of the field is modulated by using a segmentation algorithm, transforming the fluence map calculated by the treatment planning system into a number of deliverable beam segments.[1,2] The multi-leaf collimator (MLC) in the head of the linear accelerator (linac) is used to generate these irregular and sometimes small segmental fields for the delivery of IMRT. Therefore, the calculated and delivered dose for the IMRT field will depend on the specific MLC leaf

Correspondence to: Dr James Chow, Radiation Medicine Program, Princess Margaret Hospital, 610 University Avenue, Toronto, ON, Canada M5G 2M9. Tel: +416 946 4501 x5089; Fax: +416 946 6566; E-mail: james.chow@rmp.uhn.on.ca

characteristics such as the leaf end curvature, inter-leaf leakage, inter-bank leakage and the tongue-and-groove design (intra-leaf leakage) of the leaves.[3–8] In this paper, inter-leaf leakage means the leakage within a leaf or leaves (i.e. leaf transmission). Inter-bank leakage is the leakage between two opposite leaves, and intra-leaf leakage is the leakage between two leaves in the same bank. To calculate the dose accurately for the IMRT, it is necessary to consider the above factors seriously during the commissioning of the treatment planning system.[9–12]

In the Varian 21 EX linac (Varian Medical System, Palo Alto, CA), the MLC is positioned as a tertiary system below the adjustable jaws. Each MLC leaf has a rounded end with a linear trajectory, which greatly simplifies the mechanics so that failures should occur less frequently. Every leaf in the Varian MLC also has a tongue-and-groove design to minimize leakage between adjacent leaves. Such a design allows the tongue of one leaf to transverse the same space as the groove of its neighboring leaf so as to minimize the dose due to leakage between leaves.[5] Unfortunately, most treatment planning systems still have not considered the above design characteristics of MLC leaves in their dose calculation algorithms.[12,13] In IMRT, leaf leakage is a big concern in the treatment dose delivery accuracy and radiation safety.[14] It is necessary to model this unwanted stray radiation using the treatment planning system.

Recently, a new version, v7.4f, of Pinnacle treatment planning system software has been released (Philips Radiation Oncology Systems, Milpitas, CA). Unlike the old version, v6.x, which did not accurately model the rounded leaf ends, inter-leaf, inter-bank and tongue-and-groove leakage of the MLC of Varian linacs,[15] v7.4f supports corrections for the above leaf designs and characteristics.[16] In addition, v7.4f has the following new physics features: separate specification of X and Y jaw transmission, consideration of head scatter from the most limiting collimator (jaws or MLC), and improvements to the calculation accuracy of out-of-field and electron contamination dose for the MLC fields.

In this study, the physics improvements of the rounded leaf end, tongue-and-groove structure, inter-leaf and inter-bank leakage corrections as new features of v7.4f were focused on and verified. There are a number of specific modeling parameters in the commissioning of this treatment planning system and their inter-play can have significant effect on the calculation accuracy. However, this study is to compare the dose calculation accuracy between the new and old versions of Pinnacle using measurements for specific small MLC fields, rather than to explain and discuss the significant parameters and their possible effect on calculations. Small 1×1 cm^2 MLC test fields with different jaw sizes were therefore designed which helped in verifying the dosimetry due to the leaf transmission, tongue-and-groove design and inter-bank leakage. A Varian 21 EX linac with 120-leaf Millennium MLC was used and the measurements were carried out using a big scanning water tank with photon diode. Dose profiles and depth doses for the test fields were then calculated by the Pinnacle v6.2b and v7.4f for comparison with the measured profiles. The aim of this study is to investigate the physics improvements of v7.4f regarding the dose calculation for a MLC field compared to the older v6.2b.

MATERIALS AND METHODS

Physics in the dose calculation algorithm

A convolution superposition dose algorithm is used in the Pinnacle to calculate the dose.[17,18] The algorithm included creating an incident energy fluence map for the beam involved in the modeling of the MLC and the scattered radiation from the linac head. The MLCs are modeled by constructing an effective fluence matrix varied with the presence and transmission of the MLC leaf, the tongue-and-groove effects and the rounded leaf ends. When the tongue-and-groove is at the field edge, the transmission is calculated for 1/2 of the leaf thickness. In the gap between two leaves, a specified leakage transmission is applied over the tongue-and-groove width. The product of the effective MLC transmission matrix and the incident energy fluence matrix therefore incorporates the presence of the MLC. For the scattered radiation from the linac head, a model based on the two-dimensional Gaussian distribution at the position of the flattening filter in the linac head was used. Applying the Gaussian head scatter model yields accurate head scatter

https://doi.org/10.1017/S1460396906000161 Published online by Cambridge University Press

prediction for the MLC fields without requiring output factors derived from the MLC shapes. When the incident energy fluence was accurately obtained according to the MLC field, the energy fluence was used to calculate the TERMA. Then the superposition is performed to determine the dose distribution of the treatment plan.

MLC test fields

The Varian 120-leaf Millennium MLC system contains two carriages, each holding 60 leaves, with the 40 inner leaves each having a width of 0.5 cm at the isocenter. The width of the outer leaves is 1 cm and therefore all 60 leaves can generate a maximum square field size of $40 \times 40\,cm^2$ at the isocenter. In this study, three different MLC test fields were designed using the Varian SHAPER program version 6.3 (Varian Medical System, Palo Alto, CA). Figure 1(a) shows a small MLC field of $1 \times 1\,cm^2$ with the X and Y jaw set at $40 \times 1\,cm^2$. The horizontal broken line in the figure represents the dose profiles to be measured and calculated along the cross-line axis (between X1 and X2 jaw) at different depths. The measured dose profile can verify the inter-leaf leakage/tongue-and-groove design along the gap between the longitudinal edges of two leaves. Figure 1(b) shows another $1 \times 1\,cm^2$ test field same as Figure 1(a) but the X and Y jaws were changed to $1 \times 40\,cm^2$. The dose profiles (vertical broken line) to be measured and calculated were along the in-line axis (between Y1 and Y2 jaw) at different depths. Such measured dose profiles can help in verifying the intra-bank leakage through the junctions between two opposite rounded leaf ends in the MLC field. Figure 1(c) shows a test field with the X and Y jaws at $35 \times 35\,cm^2$. The broken diagonal line shows the measured/calculated dose profile, which can help in verifying the leaf transmission and tongue-and-groove design of the leaves. The reason to use jaw size smaller than $40 \times 40\,cm^2$ was due to the limited dimension of the scanning water tank ($50 \times 50 \times 50\,cm^3$) when measuring dose profiles in a deep depth such as 10 cm. The computer files of the above three test fields were sent to the linac computer with the MLC workstation program and the Varian Varis system version 7.0 (Varian Medical System, Palo Alto, CA) prepared for the measurement.

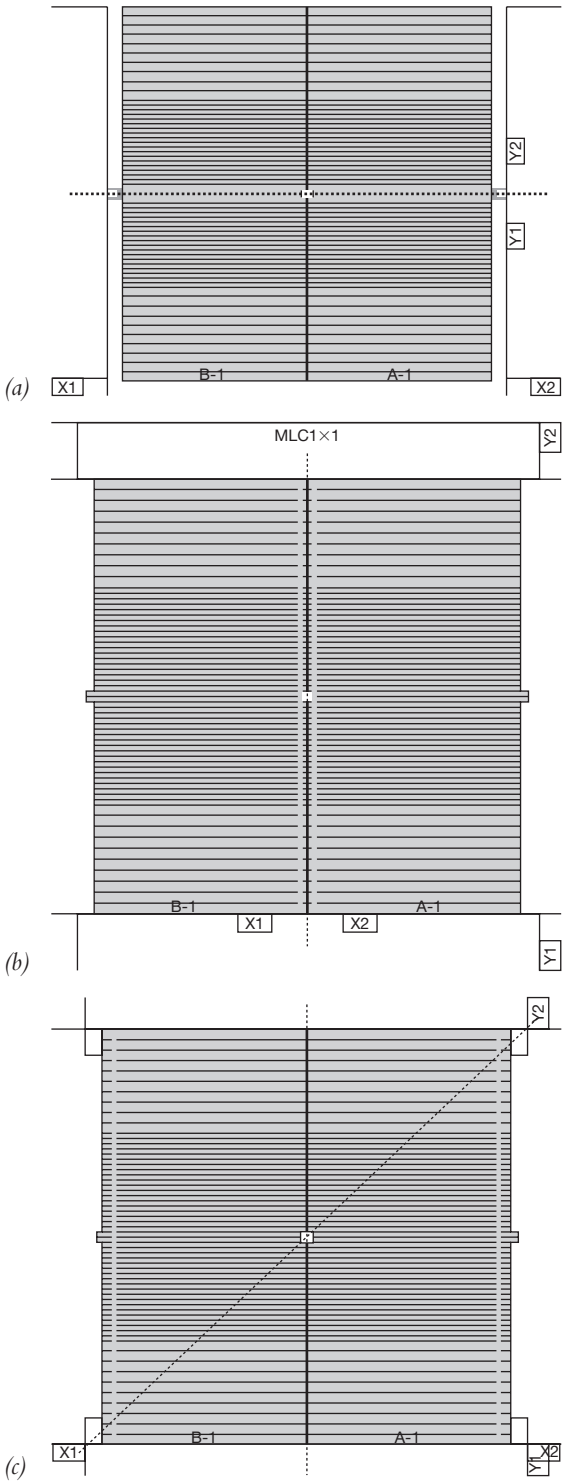

Figure 1. The three test MLC fields taken from the SHAPER program with sizes of $1 \times 1\,cm^2$ and different jaw settings: (a) X jaw = 40 cm and Y jaw = 1 cm, (b) X jaw = 1 cm and Y jaw = 40 cm and (c) X jaw = 35 cm and Y jaw = 35 cm. The broken lines represent the beam profiles to be measured/calculated at depths d_{max}, 5 cm and 10 cm using the 6 MV photon beam.

https://doi.org/10.1017/S1460396906000161 Published online by Cambridge University Press

Dose profile measurements

The dose profiles as mentioned in the above section were measured using a big scanning water tank system (RFA 300, Scanditronix Medical AB) generally used for linac commissioning. The water tank was controlled by software (Omni Pro 6) so that the dose profile with the required sampling resolution (0.5–2 mm in this study), length and orientation could be measured by a servo motor system. A photon diode (Scanditronix Medical AB, PDF-3G) was used to measure the dose profile of the small field because of its small active sampling area and thickness (2 mm and 60 μm respectively). The accuracy of the diode was established by measuring the MLC-shaped dose profiles and comparing these measurements to film and an ionization chamber.[16] The position of the water surface was determined by noting the dose variation in the diode reading at the water–air interface in the measurement. The dose profiles were measured with the highest sampling resolution and slowest speed. All measurements were carried out using a source to surface distance (SSD) of 100 cm. These measurements were carefully repeated one by one within the same day. It was found that the repeated scan agreed with the original within ±0.5%. The SSD and zero-water-level were checked frequently in order to prevent any physical effects, such as evaporation, from introducing measurement error. Since the test fields were too small to put a reference detector on the beam path, the reference dose signal was obtained from the internal monitoring ionization chamber within the gantry head of the linac.[13] Only 6 MV energy photon beam was used in this study. The dose profiles shown in Figure 1(a)–(c) were measured at depths 1.5 cm (d_{max}, depth of maximum dose for 6 MV photon beam), 5 cm and 10 cm. The water surface in the water tank was set at source to surface distance equal to 100 cm.

Pinnacle treatment planning systems

Both Pinnacle version 6.2b and 7.4f were commissioned following the Pinnacle[3] Physics Guide and Beam Data Collection Guide with respect to its versions,[19] which were used to calculate the beam profiles and penumbrae in this study. Compared to the commissioning of version 6.2b, version 7.4f required additional information of the radius of curvature of the leaf edge (8 cm) and the MLC transmission factors of gap between two leaves in the parallel (~2.2%) and opposite direction (~33.4%). Beam characteristics such as percent depth doses and beam profiles for fields up to $1 \times 1\,cm^2$ were measured for the IMRT commissioning. Big scanning water tank system (RFA 300, Scanditronix Medical AB) controlled by the software (Omni Pro 6) was used in the commissioning. The dose profile with the required sampling resolution, length and orientation could be measured by a computer controlled servo motor system. Photon diode (Scanditronix Medical AB, PDF-3G) and RK ionization chamber (Scanditronix Medical AB, RK8304) were used in the measurement for the photon beam. The commissioning of the planning system ensured the IMRT calculations result in an accurate prediction of output factors for small fields up to $1 \times 1\,cm^2$ which is essential for IMRT delivery.

The three test fields designed in Section "physics in the dose calculation algorithm" were imported to the Pinnacle treatment planning system for the dose calculations. A virtual water tank with dimension $50 \times 50 \times 50\,cm^3$ was constructed in the planning. The beam settings and arrangements in the measurement were the same ones used in the planning systems to calculate the profiles and depth doses. The grid size of dose in the calculation was set at $0.4 \times 0.4 \times 0.4\,cm^3$. This is the typical grid size being used in the prostate planning clinically. Adaptive convolution algorithm was used to calculate the dose. The algorithm is a convolution superposition approach implemented in Pinnacle to decrease the computation time by a factor of 2–3 without compromising the accuracy of the convolution superposition calculation in the inhomogeneous medium. The increase of computing speed is achieved by adaptively varying the resolution of the dose computation grid depending on the curvature of the TERMA and the dose distribution. The calculation region of interest specified by Pinnacle was set to be as big as the virtual water tank.

RESULTS

Figure 2(a)–(c) show the measured and calculated dose profiles for the test field as shown in Figure 1(a) at depths d_{max}, 5 cm and 10 cm, respectively. All profiles were normalized to the maximum dose at depth d_{max}. Similarly, Figure 3(a)–(c) show dose profiles measured and calculated for the test field as

https://doi.org/10.1017/S1460396906000161 Published online by Cambridge University Press

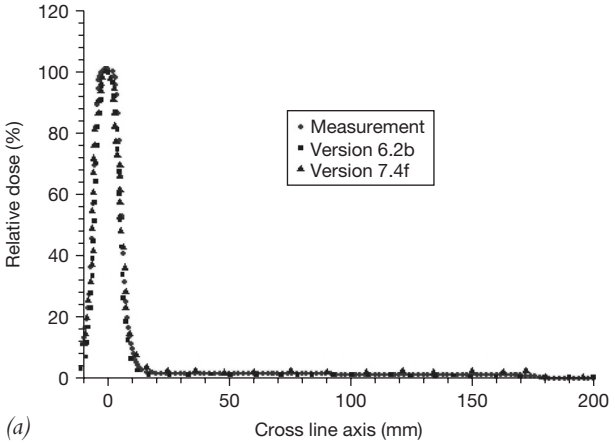

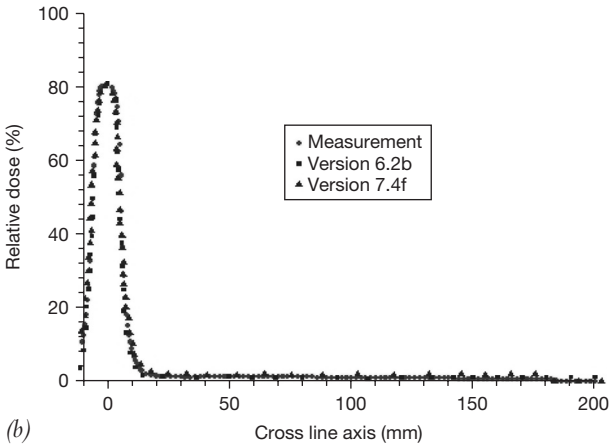

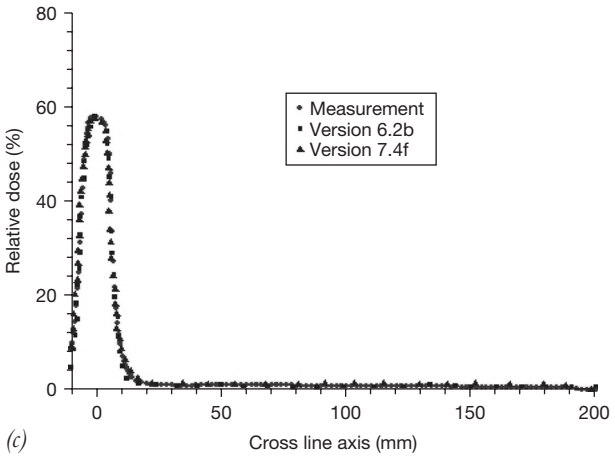

Figure 2. Beam profiles measured and calculated using Pinnacle v6.2b and v7.4f according to the test MLC field in Figure 1(a) at depths (a) d_{max}, (b) 5 cm and (c) 10 cm.

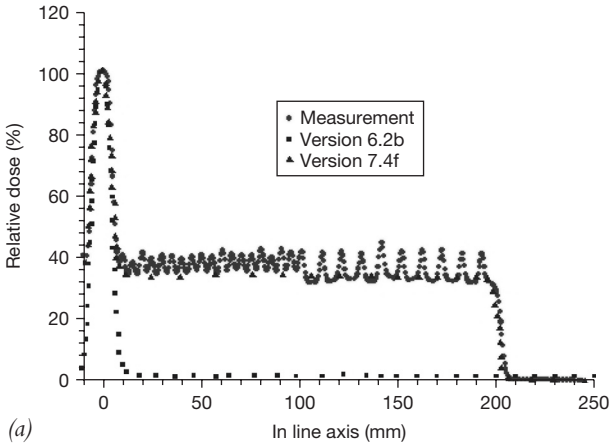

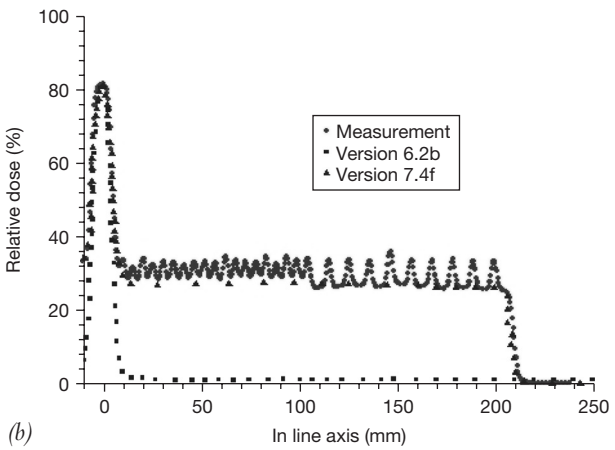

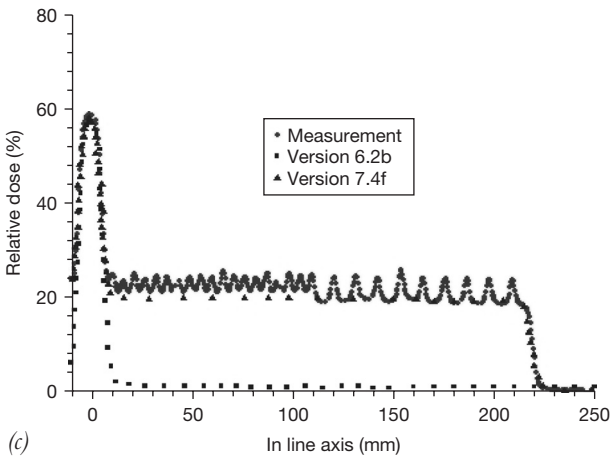

Figure 3. Beam profiles measured and calculated using Pinnacle v6.2b and v7.4f according to the test MLC field in Figure 1(b) at depths (a) d_{max}, (b) 5 cm and (c) 10 cm.

shown in Figure 1(b) at depths d_{max}, 5 cm and 10 cm respectively, and Figure 4(a)–(c) show dose profiles at different depths according to test field in Figure 1(c). Similar to Figure 2, all profiles in Figures 3 and 4 were normalized to the maximum dose at depth d_{max}. Table 1 shows the percentage depth doses of Figures 2–4 measured and calculated at the central beam axis (CAX) at depths 5 cm and 10 cm.

https://doi.org/10.1017/S1460396906000161 Published online by Cambridge University Press

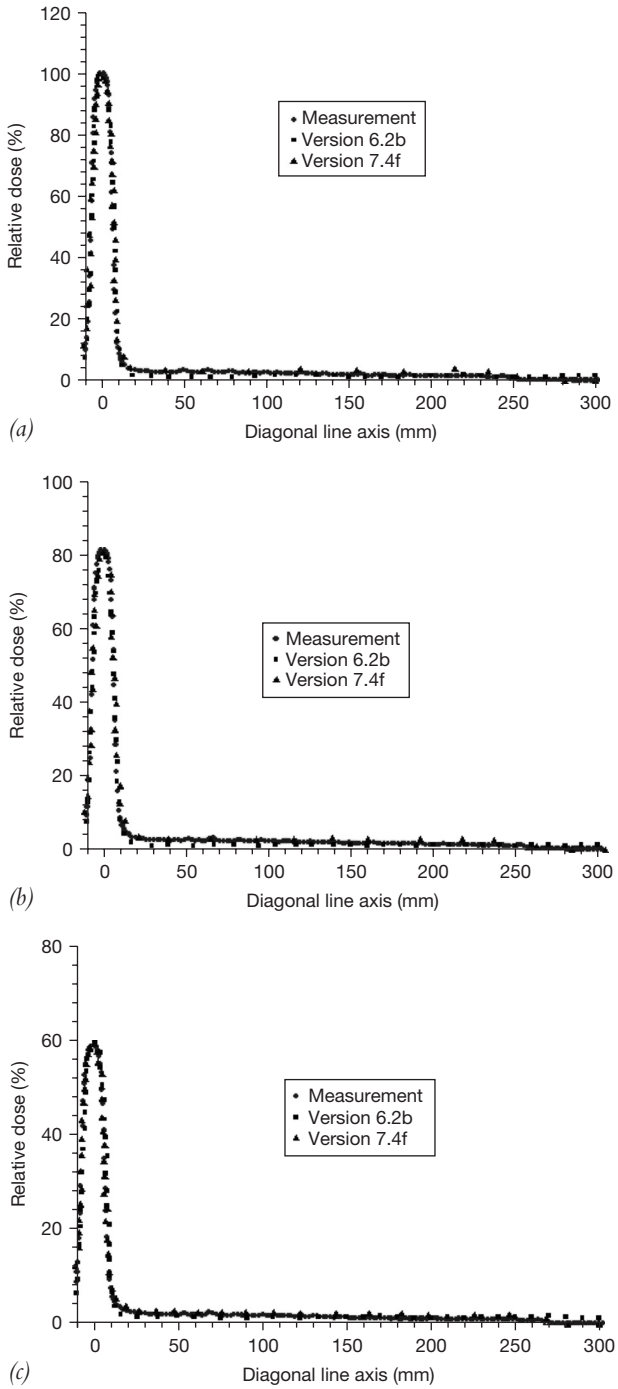

Figure 4. Beam profiles measured and calculated using Pinnacle v6.2b and v7.4f according to the test MLC field in Figure 1(c) at depths (a) d_{max}, (b) 5 cm and (c) 10 cm.

DISCUSSION

Dose profiles verifying the inter-leaf leakage/tongue-and-groove design

In Figure 2(a), the dose profiles were measured and calculated at the gap between two longitudinal edges of MLC leaves along the cross-line axis. The part of profile beyond the $1 \times 1\,cm^2$ field edge represents the leakage from the inter-leaf/tongue-and-groove effect. It can be seen that the dose profiles measured in this region is varying between 1% and 3%, which agree well with those calculated by Pinnacle v6.2b and v7.4f. Similar results can be observed in Figure 2(b) and (c). It shows that Pinnacle v6.2b performed equally well as v7.4f in calculating the dose profiles along the gap between two leaves with the jaws opened. However, with the jaws moved to $1 \times 1\,cm^2$, the measured and calculated profiles in such region were found to be very near to zero, because the jaws provide additional attenuation of the beam that dramatically reduces leakage. On the other hand, when the dose at the junction between two opposite leaves was measured, the inter-bank leakage was serious due to the rounded leaf ends. This can be seen in Figure 3 showing the in-line axis dose profiles at different depths.

Dose profiles verifying the intra-bank leakage

In Figure 3(a), the part of measured profile beyond the field edge was seen to vary between about 35.4% and 42.1% in the inner leaf (width of leaf = 0.5 cm) region, and 32.8% and 42.3% in the outer leaf (width of leaf = 1 cm) region. The ripples in the "zigzag" profile were understood as the increase of doses due to the differential leakage through the rounded ends of opposing bank leaves that are abutting. In Figure 3(b) and (c), similar dose variations were measured to be 28.9–33.5% and 21.4–25.0% in the inner leaf region respectively, and 27.1–34.4% and 19.2–24.3% in the outer leaf region respectively. The decrease of dose from Figure 3(a)–(c) was due to the beam attenuation according to the percentage depth dose, and it can be seen that the relative ripple with respect to the CAX dose reduces more from 5 cm to 10 cm than from 1.5 cm to 5 cm. For the same profile region in Figure 3, the doses calculated using Pinnacle v6.2b varied between about 1% and 2%, which were the same as in Figure 2. However, such large

https://doi.org/10.1017/S1460396906000161 Published online by Cambridge University Press

Table 1. Percentage depth doses of Figures 2–4 measured and calculated at the central beam axis at depths 1.5 cm (d_{max}), 5 cm and 10 cm

Depth (cm)	Field size = 40 × 1 cm² Figure 1(a)			Field size = 1 × 40 cm² Figure 1(b)			Field size = 35 × 35 cm² Figure 1(c)		
	Measurement (%)	v6.2b (%)	v7.4f (%)	Measurement (%)	v6.2b (%)	v7.4f (%)	Measurement (%)	v6.2b (%)	v7.4f (%)
d_{max}	100.0	100.0	100.0	100.0	100.0	100.0	100.0	100.0	100.0
5	80.4	80.5	80.2	80.1	80.0	80.6	80.5	80.1	80.0
10	58.3	58.0	57.9	57.8	57.5	57.7	58.8	58.7	58.5

deviation between the measured and calculated dose was greatly improved in v7.4f. The doses calculated by v7.4f in Figure 3(a)–(c) were 34.3%, 27.7% and 19.7% in the profile region beyond the field edge respectively, and it can be seen that the calculated doses at different depths were near to the lower bound of the fluctuated doses from the measurement. However, due to the limited resolution of the grid size ($0.4 \times 0.4 \times 0.4\,cm^3$) compared to the leaf width of 0.5 cm, the "zigzag" feature in the profile is burred out due to interpolation. Smaller grid size of $0.15 \times 0.15 \times 0.15\,cm^3$ has been tried in the calculation with a very slow computing speed, but the calculated dose profile is very similar to that using a larger grid size of $0.4 \times 0.4 \times 0.4\,cm^3$. Only when the grid size was reduced to $0.05 \times 0.05 \times 0.05\,cm^3$, the "zigzag" feature would appear. In such calculation, the regional of interest had to be reduced from the size of the whole big water tank in order to save the dose calculation time. It can be seen that if the computing speed is fast enough to support such a high calculation resolution as used in the measurement, the planning system is able to calculate the correct dose. However, in reality, using such high calculation resolution is still not practical because the computing time is unreasonably long. Therefore in this study, only the grid size used clinically is used in the comparison.

Dose profiles verifying the leaf transmission and tongue-and-groove design

Figure 4 shows the diagonal dose profiles of a $1 \times 1\,cm^2$ field with X and Y jaw of $35 \times 35\,cm^2$ at different depths. In addition to the tongue-and-groove structure, which has been verified in Figure 2, Figure 4 also verified the beam transmission of the whole thickness of leaves. The results show that the measured profiles beyond the field edges were between 1% and 3%, and both v6.2b and v7.4f could calculate doses agreed well with the measurements with error bar ±1%. Table 1 shows the percentage depth doses for the three test fields at depths 5 cm and 10 cm. It can be seen that accurate depth doses for the test fields as shown in Figure 1(a)–(c) were calculated by Pinnacle v6.2b and v7.4f with error bar within ±1%. It seems that the inter-bank leakage observed in Figure 3 does not affect the calculations of percentage depth doses. The design of the tongue-and-groove is intended to ensure that a similar attenuation is achieved, when neighboring leaves are aligned, than that seen under the body of a leaf. Our results show that this is achieved.

CONCLUSIONS

The improved peripheral dose profile accuracy in the newly released Pinnacle software (v7.4f), that supporting modeling of the MLC rounded leaf ends, tongue-and-groove structure and inter-leaf leakage, was verified in this study, focusing on the leakages between leaves along the cross-line, in-line and diagonal axis in a small MLC field. Three test fields were designed so that different measured dose profiles in the fields at different depths could verify the leaf leakage along the cross-line axis between two leaves (tongue-and-groove design), the leaf leakage along the in-line axis between two groups of leaves (junctions of two rounded leaf ends), and the leaf leakage along the diagonal axis of closed leaves (tongue-and-groove design and the leaf transmission). The measured results using a big scanning water tank and photon diode were compared to those calculated by Pinnacle v6.2b and v7.4f. It is found that both

https://doi.org/10.1017/S1460396906000161 Published online by Cambridge University Press

versions performed well in calculating the dose profiles along the cross-line and diagonal axis. However, for the in-line axis profiles along the junctions of two opposite groups of leaves, v6.2b did not model the inter-bank leakage well, while v7.4f predicted a relative dose equal to 34.3% in the region beyond the MLC field edge at depth d_{max}. Although the shape of the calculated profile is different from the measurement, which varied between 35.4% and 42.1%, v7.4f can basically determine the inter-bank leakage in the dose profile. In addition, both Pinnacle v6.2b and v7.4f performed well in calculating the percentage depth doses for the small MLC fields with different jaw sizes.

ACKNOWLEDGMENTS

The authors would like to thank all the physics staff for contributing to the commissioning of the Pinnacle v6.2b and 7.4f system. Authors would also like to thank Melanie Seguin and Andrew Alexander for helping in some of the measurements. All measurements in this work were carried out in the Grand River Regional Cancer Center.

References

1. Boyer A, Biggs P, Galvin J, Klein E, LoSasso T, Low D, Mah K, Yu C. Basic applications of multileaf collimators. Report of the AAPM Radiation Therapy Committee Task Group No. 50 Medical Physics, 2001.
2. Bar W, Alber M, Nusslin F. A variable fluence step clustering and segmentation algorithm for step and shoot IMRT. Phys Med Biol 2001; 46:1997–2007.
3. Wang X, Spirou S, LoSasso T, Stein J, Chui CS, Mohan R. Dosimetric verification of intensity-modulated fields. Med Phys 1996; 23:317–327.
4. LoSasso T, Chui CS, Ling CC. Physical and dosimetric aspects of a multileaf collimation system used in the dynamic mode for implementing intensity modulated radiotherapy. Med Phys 1998; 25:1919–1927.
5. Van Stanvoort JPC, Heijmen BJM. Dynamic multileaf collimation without "tongue-and-groove" underdosage effects. Phys Med Biol 1996; 41:2091–2105.
6. Boyer AL, Li S. Geometric analysis of light-field position of a multileaf collimator with curved ends. Med Phys 1997; 24:757–762.
7. Das IJ, Desobry GE, McNeeley SW, Cheng EC, Schultheiss TE. Beam characteristics of a retrofitted double-focused multileaf collimator. Med Phys 1998; 25:1676–1684.
8. Arnfield MR, Siebers JV, Kim JO, Wu Q, Keall PJ, Mohan R. A method for determining multileaf collimator transmission and scatter for dynamic intensity modulated radiotherapy. Med Phys 2000; 27:2231–2241.
9. Van Esch A, Bohsung J, Sorvari P, Tenhunen M, Paiusco M, Iori M, Engstrom P, Bystrom H, Huyskens DP. Acceptance tests and quality control (QC) procedures for the clinical implementation of intensity modulated radiotherapy (IMRT) using inverse planning and the sliding window technique: experience from five radiotherapy departments. Radiother Oncol 2002; 65:53–70.
10. Ezzell GA, JGalvin JM, Low D, Palta JR, Rosen I, Sharpe MB, Xia P, Xiao Y, Xing L, Yu CX. Guidance document on delivery treatment planning, and clinical implementation of IMRT: report of the IMRT subcommittee of the AAPM radiation therapy committee. Med Phys 2003; 30: 2089–2115.
11. Laub WU, Wong T. The volume effect of detectors in the dosimetry of small fields used in IMRT. Med Phys 2003; 30:341–347.
12. Chow JCL, Seguin M, Alexander A. Dosimetric effect of collimating jaws for small multileaf collimated fields. Med Phys 2005; 32:759–765.
13. Chow JCL, Wettlaufer B, Jiang R. Dosimetric effects on the penumbra region of irregular multi-leaf collimated fields. Phys Med Biol 2006; 51:N31–N38.
14. Stathakis S, Price R, Ma CM. Dosimetry validation of treatment room shielding design. Med Phys 2005; 32:448–454.
15. Cadman P, Bassalow R, Sidhu NP, Ibbott G, Nelson A. Dosimetric considerations for validation of a sequential IMRT process with a commercial treatment planning system. Phys Med Biol 2002; 47:3001–3010.
16. Cadman P, McNutt T, Bzdusek K. Validation of physics improvements for IMRT with a commercial treatment-planning system. J Appl Clin Med Phys 2005; 6:74–86.
17. Mackie TR, Scrimger JW, Battista J. A convolution method of calculating dose for 15-MV x rays. Med Phys 1985; 12:188–196.
18. Papanikolaou N, Mackie TR, Meger-Wells C, Gehring M, Reckwerdt P. Investigation of the convolution method for polyenergetic spectra. Med Phys 1993; 20:1327–1336.
19. Philips Radiation Oncology Systems, Pinnacle^3 Physics Reference Guide (release 7.4): 2004.

https://doi.org/10.1017/S1460396906000161 Published online by Cambridge University Press